IOPscience iopscience.iop.org

Home Search Collections Journals About Contact us My IOPscience

# Temperature limits for ballistic quantization in a GaAs/AlGaAs one-dimensional constriction

This article has been downloaded from IOPscience. Please scroll down to see the full text article.

1993 J. Phys.: Condens. Matter 5 L559

(http://iopscience.iop.org/0953-8984/5/44/003)

View the table of contents for this issue, or go to the journal homepage for more

Download details:
IP Address: 171.66.16.96
The article was downloaded on 11/05/2010 at 02:09

Please note that terms and conditions apply.

J. Phys.: Condens. Matter 5 (1993) L559–L564. Printed in the UK

LETTER TO THE EDITOR

# Temperature limits for ballistic quantization in a GaAs/AlGaAs one-dimensional constriction

J E F Frost, M Y Simmons, M Pepper, A C Churchill, D A Ritchie and G A C Jones
Cavendish Laboratory, Madingley Road, Cambridge CB3 0HE, UK

Received 15 September 1993

**Abstract.** One-dimensional (1D) ballistic constrictions have been made in a two-dimensional electron gas of high carrier concentration ($6.5 \times 10^{11}$ cm$^{-2}$) and high mobility ($9.5 \times 10^5$ cm$^2$ V$^{-1}$ s$^{-1}$) formed at the interface of a GaAs/AlGaAs heterostructure. At least seven ballistic conductance steps were clearly observed at 4.2 K and remained discernible up to 40 K. A 1D subband spacing of 10 meV was found from the electric-field-induced half plateaux in differential conductance. The mobility and carrier concentration of the two-dimensional electron gas were also measured as functions of temperature in order to compare the relative effects on the degradation of the ballistic quantization of Fermi–Dirac broadening at the Fermi energy and the reduction in the ballistic mean free path. The close similarity between the experimental conductance characteristics and those calculated with a simple assumption of the Fermi–Dirac electron energy distribution strongly suggests that this is the principal mechanism in smearing the quantized conductance plateaux.

The conductance of a ballistic one-dimensional constriction in a two-dimensional electron gas (2DEG) formed by a split Schottky gate over a GaAs/AlGaAs heterostructure quantized in multiples of $2e^2/h$ was first observed at low temperatures (300 mK) [1,2]. Ballistic conductance occurs when the mean free path is much larger than the length of the split gate and the constriction width is comparable with the Fermi wavelength.

The earliest ballistic quantization experiments were made at 330 mK, but more recently ballistic transport has been studied at temperatures up to 10 K [3]. Evidence for ballistic quantization has been observed in a constriction defined by ion beam damage and with gate-controlled carrier concentration at 14.8 K [4], and in a split-gate device on a shallow 2DEG at 30 K [5]. If ballistic-type devices are to have any commercial application then operation at higher temperatures would be an advantage. Operation at liquid nitrogen temperature, 77 K, would be most convenient, but any temperature higher than 4.2 K would be beneficial because refrigeration costs decrease with an increase in temperature. The quality of the ballistic quantization conductance steps is usually taken to be a measure of the degree of ballistic transport. In this work we compare the effect on the quantized conduction due to an increase in temperature via two mechanisms: the Fermi–Dirac broadening at the Fermi energy and the reduction of the ballistic mean free path due to the temperature dependence of the electron mobility and carrier concentration.

The split gate was made by electron beam lithography and consisted of two 80% Ni:20% Cr/Au rectangular corners offset at 45° by 100 nm (inset of figure 1). The radius of curvature of the corners is estimated to be 20 nm. The GaAs/AlGaAs heterostructure comprised, from the surface, 10 nm undoped GaAs, 40 nm Si-doped AlGaAs, 10 nm

0953-8984/93/440559+06$07.50 © 1993 IOP Publishing Ltd 

undoped AlGaAs and 1 $\mu$m undoped GaAs. The mobility was $9.5 \times 10^5$ cm$^2$ V$^{-1}$ s$^{-1}$ and the sheet carrier concentration was $6.5 \times 10^{11}$ cm$^{-2}$ at 4.2 K after illumination by a red light-emitting diode. Two-terminal conductance measurements were made using lock-in techniques with a constant 100 $\mu$V AC excitation voltage.

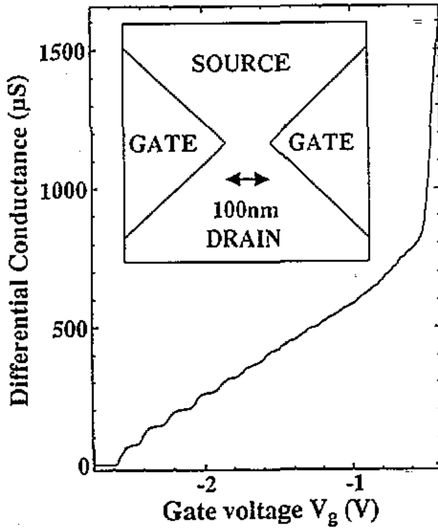


**Figure 1.** Split-gate conductance as a function of gate voltage. No series resistance correction has been made. The inset shows a schematic diagram of the device.

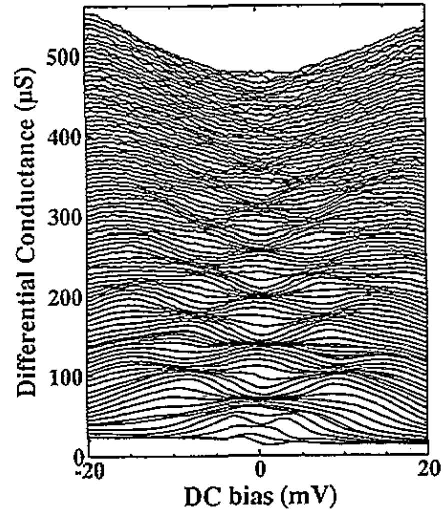


**Figure 2.** The differential conductance as a function of source–drain bias for different gate voltages. No series resistance correction has been made.

Figure 1 shows the differential conductance $G$ as a function of the gate voltage $V_g$ at 4.2 K; there are at least seven clear conductance plateaux. No correction has been made for the series resistance and this accounts for the separation of the plateaux being less than $2e^2/h$. Figure 2 shows the differential conductance as a function of the DC source–drain bias at 4.2 K; the bunching of the curves at values midway between those at zero DC bias is induced by the electric field [6]. The subband energy spacings were deduced from the positions of these half plateaux in the differential conductance at high DC bias in a similar fashion to the method described by Patel *et al* [6]. A 1D subband spacing of 10 meV for the last 1D subband decreasing to about 6 meV for the fifth 1D subband were calculated from [7]

$$\Delta E(n, n+1) = (e/2)(V_1 + V_2) \tag{1}$$

where $\Delta E(n, n+1)$ is the energy separation between the bottoms of the $n$th and $(n+1)$th 1D subbands, and $V_1$ and $V_2$ are the negative and positive source–drain voltages respectively at which the curves bunch at a conductance value midway between conductance plateau values at zero DC bias. The value of $\hbar\omega_y$ between the last two subbands was entered as a parameter in the numerical calculation. Figure 3 shows the Hall measurements as a function of temperature up to 80 K. The mobility drops by a factor of three and the carrier concentration by 20% from the 4.2 K values.

The electrostatic potential of a 1D constriction in a 2DEG resembles a saddle point, where the midpoint of the constriction is a maximum in potential in the direction of travel (the $x$ direction), and a minimum in the confining lateral potential (the $y$ direction). The potential

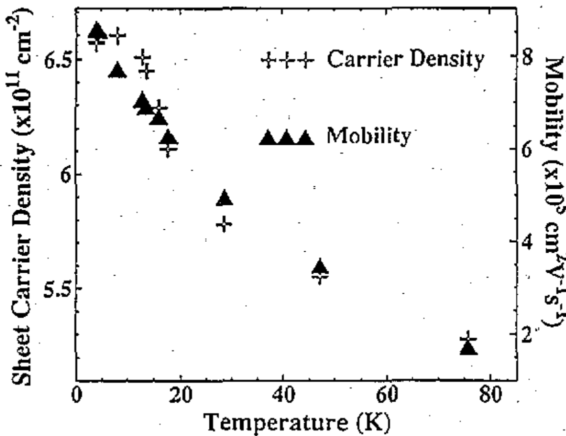


**Figure 3.** The sheet carrier density (crosses) and low-field mobility (triangles) as a function of temperature for a 2DEG Hall bar without a split-gate device.

barrier and the confining potential are both most simply assumed to be parabolic in shape, leading to the following equation for the potential [8]:

$$V(x, y) = V_0 - \tfrac{1}{2}m\omega_x^2x^2 + \tfrac{1}{2}m\omega_y^2y^2. \tag{2}$$

The transmission probability through the constriction from 1D subband $m$ to $n$ is given by [8]

$$T_{mn} = \delta_{mn}\left[1 + \exp(-\pi\varepsilon_n)\right] \tag{3}$$

where $\delta_{mn}$ is the Krönecker delta and

$$\varepsilon_n = \left[E - \hbar\omega_y\left(n + \tfrac{1}{2}\right) - V_0\right]/(\hbar\omega_x). \tag{4}$$

The conductance, $G(E, T)$, is given by

$$G(E_F, T) = \int_0^\infty G(E, T = 0)\left(-\partial f(E_F, E)/\partial E\right) dE \tag{5}$$

where $f(E_F, E)$ is the Fermi–Dirac function

$$f(E_F, E) = \left\{1 + \exp\left[(E - E_F)/kT\right]\right\}. \tag{6}$$

The saddle point model is most applicable when there are few 1D subbands, and the device approaches pinch-off. For larger numbers of 1D subbands, with $n$ more than about 6, the parabolic potential is flattened at the bottom by the screening effect of conduction electrons in the constriction [9]. This leads to the decrease in subband spacing with increasing conductance described above and explains why, at a given temperature, the lowest conductance plateau is always better defined than those at higher conductance. The flattening at the bottom of the well is not taken into account in our model and hence it fails to predict the decrease in step quality with increasing 1D subband index. The abruptness of the steps at temperatures low enough to give minimal thermal smearing is determined

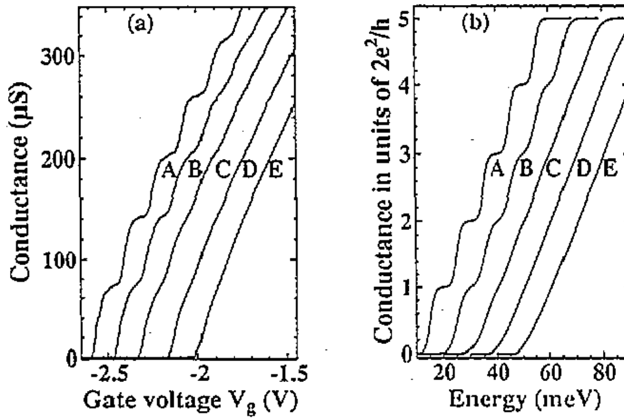


**Figure 4.** (a) The experimental conductance as a function of gate voltage for five different temperatures, 4.2, 12.9, 22.9, 31.6 and 42.7 K (labelled A–E). No series resistance correction has been made. The temperature labels are the same as for figures 4(b), 5(a) and 5(b). (b) The calculated conductance as a function of energy.

in this model by the ratio $\omega_y/\omega_x$ [8]. This condition was met for our sample at 4.2 K, so these data were fitted to the theoretical conductance to obtain $\omega_y/\omega_x \simeq 2$, a value similar to that found by Martin-Moreno *et al* [10].

The conductance as a function of temperature was obtained by firstly applying equation (3) to find the conductance of one 1D subband and then summing five of these curves, offset each time by the 1D subband spacing. These data were then numerically convolved with the Fermi–Dirac function at temperatures of 4.2, 12.9, 22.9, 31.6 and 42.7 K, the same temperatures as the experimental data. Figure 4 shows the experimental and calculated conductance for these five temperatures. The curves are offset for clarity and the scales have been chosen to normalize the conductance steps and equate the applied gate voltage with the effective energy scale. Figure 5 shows the derivative of the experimental and calculated conductance data. The number of discernible minima in the derivatives, corresponding to steps in conductance, decreases steadily with an increase in temperature. The derivative of the first step in conductance may be enhanced by the rapid change in conductance as the device reaches pinch-off.

We measured a 1D subband spacing of 10 meV, similar to that estimated for the device of Snider *et al* [5] with a similar carrier concentration, even though our 2DEG is at twice the depth (60 nm compared with 30 nm). An advantage of the greater 2DEG depth is that it is easier to obtain higher electron mobilities as the depth increases [11]. We believe that the sharp corners and narrow width (100 nm) of our device yield a very short constriction, less than 200 nm long, with steep potential walls, leading to a large 1D subband spacing. Table 1 shows the transport properties of previous work [4, 5] compared with our results. Measurement temperature, carrier density $n_s$, mobility $\mu$, mean free path and constriction length are given. The mean free path is given by $l = v_F\tau$ where $v_F$ is the Fermi velocity and $\tau$ is the electron scattering time. In terms of $\mu$ and $n_s$, $1 = (\hbar/e)\mu\sqrt{2\pi n_s}$. In all cases, even in our sample at 40 K, the mean free path is at least an order of magnitude greater than the constriction length, and this implies that the decrease in mean free path is not the cause of the degradation of the ballistic quantization with an increase in temperature in these very short devices.

The close similarity between the experimental conductance characteristics and those calculated with a simple assumption of the Fermi–Dirac electron energy distribution strongly

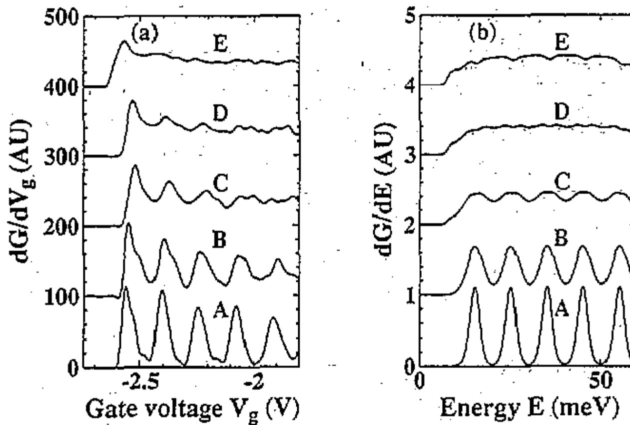


**Figure 5.** (a) The derivative of the experimental conductance with respect to gate voltage as a function of gate voltage. (b) The derivative of the calculated conductance with respect to energy as a function of energy.

**Table 1.** Electrical transport properties of samples from previous work [4, 5] and from the present study.

| | Temperature (K) | $n_s$ ($10^{11}$ cm$^{-2}$) | $\mu$ ($10^5$ cm$^2$ V$^{-1}$ s$^{-1}$) | $l$ ($\mu$m) | Length (nm) |
|---|---|---|---|---|---|
| Snider *et al* [5] | 4.2 | 5 | 2.9 | 3.4 | 200 |
| Hirayama *et al* [4] | 11 | 3 | 3.8 | 3.4 | 300 |
| Current work | 4.2 | 6.6 | 9.5 | 12.7 | 200 |
| Current work | 40 | 5.7 | 4 | 5.0 | 200 |

suggests that this is the principal mechanism in smearing the quantized conductance plateaux [12].

Therefore, absence of 1D plateaux does not mean that ballistic transport is not taking place, but that its presence must be verified by a different method. Further work is needed to determine the ballistic mean free path as a function of temperature, possibly using techniques described by Molenkamp *et al* [3].

We would like to acknowledge the financial support of the SERC and technical support from D Heftel, T Jobson and S Gymer. JEFF would like to thank S R Andrews, J T Nicholls, C J B Ford and I Zailer for many useful discussions. DAR would like to acknowledge support from Toshiba Cambridge Research Centre Ltd.

## References

[1] Wharam D A, Thornton T J, Newbury R, Pepper M, Ahmed H, Frost J E F, Hasko D G, Peacock D C, Ritchie D A and Jones G A C 1988 *J. Phys. C: Solid State Phys.* **21** L209–14

[2] van Wees B J, van Houten H, Beenakker C W J, Williamson J G, Kouvenhoven L P, van der Marel D and Foxon C T 1988 *Phys. Rev. Lett.* **60** 848

[3] Molenkamp L W, Brugmans M J P, van Houten H and Foxon C T 1992 *Semicond. Sci. Technol.* **7** B228–30

[4] Hirayama Y and Saku T 1989 *Appl. Phys. Lett.* **54** 2556–8

[5] Snider G L, Miller M S, Rooks M J and Hu E L 1991 *Appl. Phys. Lett.* **59** 2727–9

[6] Patel N K, Nicholls J T, Martin-Moreno L, Pepper M, Frost J E F, Ritchie D A and Jones G A C 1991 *Phys. Rev.* B **44** 549–55

[7] Zagoskin A M 1990 *Pis. Zh. Eksp. Teor. Fiz.* 52 1043 (Engl Transl. 1991 *JETP Lett.* 52 435)
[8] Büttiker M 1990 *Phys. Rev.* B **41** 7906–9
[9] Laux S E, Frank D J and Stern F 1988 *Surf. Sci.* **196** 101–6
[10] Martin-Moreno L, Nicholls J T, Patel N K and Pepper M 1991 *J. Phys.: Condens. Matter* **4** 1323–33
[11] Harris J J, Foxon C T, Barnham K W J, Lacklison D E, Hewett J and White C 1987 *J. Appl. Phys.* **61** 1219–21
[12] Bagwell P F and Orlando T P 1989 *Phys. Rev.* B **40** 1456